STRAIN RATE AND DYNAMIC FRACTURING IN PLANETARY-SCALE IMPACTS. C. M. Ernst[1], O. S. Barnouin-Jha[1], K. T. Ramesh[2], P. K. Swaminathan[1], and J. Kimberley[2], [1]Johns Hopkins University Applied Physics Laboratory, Laurel, MD 20723 (carolyn.ernst@jhuapl.edu), [2]Johns Hopkins University, Department of Mechanical Engineering, Baltimore, MD 21218.

Introduction: Impacts initiate dynamic fracturing on macro-and micro-scales, and the resulting fragmentation can be related to strain rate. The dynamic fracture process has been directly observed at low strain rates (~10^{-2} to 10^{-3} s^{-1}, during earthquakes) and at high strain rates (~10^{5} to 10^{6} s^{-1}, during laboratory-scale hypervelocity impact experiments) [1]. Based on first order estimates of the strain rate in the projectile (~ impact velocity/projectile diameter) [2], the strain rates encountered during a typical planetary-scale impact range from ~10^{0} to 10^{2} s^{-1}. These intermediate values lie within an strain rate regime that is extremely difficult to observe naturally. Using numerical simulations and new dynamic fragmentation models, we investigate what strain rates might be generated during large scale impacts and assess implications for fragmentation considering new dynamic fragmentation models.

Fragmentation Models: To first order, higher strain rates yield smaller fragment sizes. However, in reality the relationship is more complex. Experiments [3] have found that classical energy models of dynamic fracture (e.g., Grady-Kipp [4]) overestimate the average fragment size produced for a given strain rate. Observations of lunar craters report large amounts of very fine fragments, more so than would be predicted by classical models [5]. This indicates that the classical models are not accounting for important factors.

In fragmentation modeling, it is important to account for residual kinetic energy associated with crack dynamics. A recent analytical-numerical model (ZMR) incorporated the elastic wave propagation, crack nucleation, growth, and interactions into the analysis. Here, kinetic energy is extracted from the system and applied to additional fracturing, creating new cracks and resulting in smaller fragment sizes [6]. This effect is pronounced at intermediate to low strain rates, and allows this model to predict fragment sizes in closer agreement to experimental observations [3,7].

Figure 1 compares the normalized average fragment size to the strain rate for basalt. The expected strain rate regimes for earthquakes, planetary-scale impacts, and laboratory-scale impacts are indicated. At high strain rates, the two models differ by approximately an order of magnitude. A significant turnover in average fragment size is observed between ~10^{4} to 10^{5} s^{-1}. Predictions using classical fragmentation models can overestimate the average fragment size by as much as several orders of magnitude at intermediate to low strain rates.

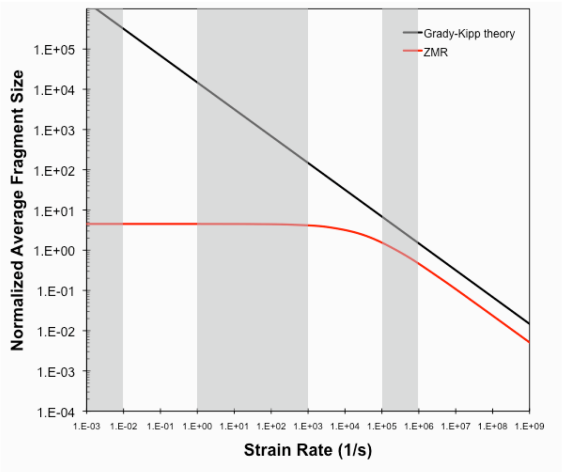

Figure 1. Comparison of two fragmentation models, adapted from [6]. The black line represents the classical Grady-Kipp theory, and the red line represents the ZMR model [6]. The shaded regions indicate the average strain rate experienced by the bulk of material involved in (a) an earthquake, (b) a planetary-scale impact, and (c) an experimental impact. There is a several order of magnitude difference in predicted normalized average fragment size between the two models for intermediate to low strain rates regimes.

Simulations: To evaluate the effect of this new dynamic fracture model for planetary-scale cratering events, we undertake numerical simulations to evaluate the strain rates a target might endure. We derive strain rates from computational calculations using the CTH shock physics analysis package [8] and implementing the built in elastic-plastic fracture model. Adaptive Mesh Refinement (AMR) [9] was implemented to maintain high resolution along shockwave boundaries. The events were modeled as quartz spheres impacting at 5 km/s and 90º into quartz targets. A range of projectile diameters were investigated: 1cm (~ laboratory-scale events), 1m, and 1km.

Results: Figure 2 illustrates the strain rates endured by the three simulated impacts at times normalized to the penetration time of the projectile. Typical strain rate values encountered by the bulk of the target were: 10^{3} to 10^{5+} for 1 cm; 10^{1} to 10^{3} for 1 m; 10^{-2} – 10^{0} for 1km. Although the relative values of these strain rates are in concert with the estimates made using the ratio of impact velocity to projectile diameter, the absolute values are lower than predicted for the bulk of the affected target material. Regions closer to the impact

point experienced strain rate values approximately an order of magnitude higher during the initial projectile penetration phase. Strain rate values at the point of impact were similar in all three cases.

The bulk of the material for the 1 cm case endures strain rates that fall into a regime close to that of the predicted regime for laboratory impacts. For the larger-scale impact simulations, low strain rates were common and high strain rates were rare. The 1 m case yielded strain rates that fall into the intermediate range predicted for planetary-scale impacts. For the 1 km case, the strain rates are even lower, between the intermediate and low (earthquake) range. Therefore, use of the correct fragmentation model is extremely important for planetary-scale impacts.

Based upon the new ZMR model (from Figure 1), we expect that planetary-scale impacts should produce significantly finer material than previously expected. We plan to investigate the effect of the fracture models incorporated into the numerical simulations on the observed target strain rates. A brittle fracture kinetics models for concrete and more complex models will be examined.

References: [1] Barnouin-Jha, O.S. et al. (2008) *LPS XXXIX, #1906*. [2] Melosh, H. J. et al. (1992) *JGR*, 97, 14735-14739. [3] Paliwal, B. et al. (2008) *Journal of the Mechanics and Physics of Solids*, 56, 896-923. [4] Grady, D. E. and Kipp, M. E. (1985) *Mechanics of Materials*, 4, 311-320. [5] Schultz, P. H. and Mendell, W. (1978) *Proc. LPS IX*, 2857-2883. [6] Zhou, F. H., et al. (2006) *Applied Physics Letters*, 88, 261918. [7] Kimberly, J. et al. (2009) *LPS* XL. [8] McGlaun, J. M. et al. (1990) *Int. J. Impact Eng.*, 10, 351-360. [9] Crawford, D. A. et al. (2002) in *New Models and Hydrocodes for Shock Wave Processes in Condensed Matter*, Edinburgh, U.K.

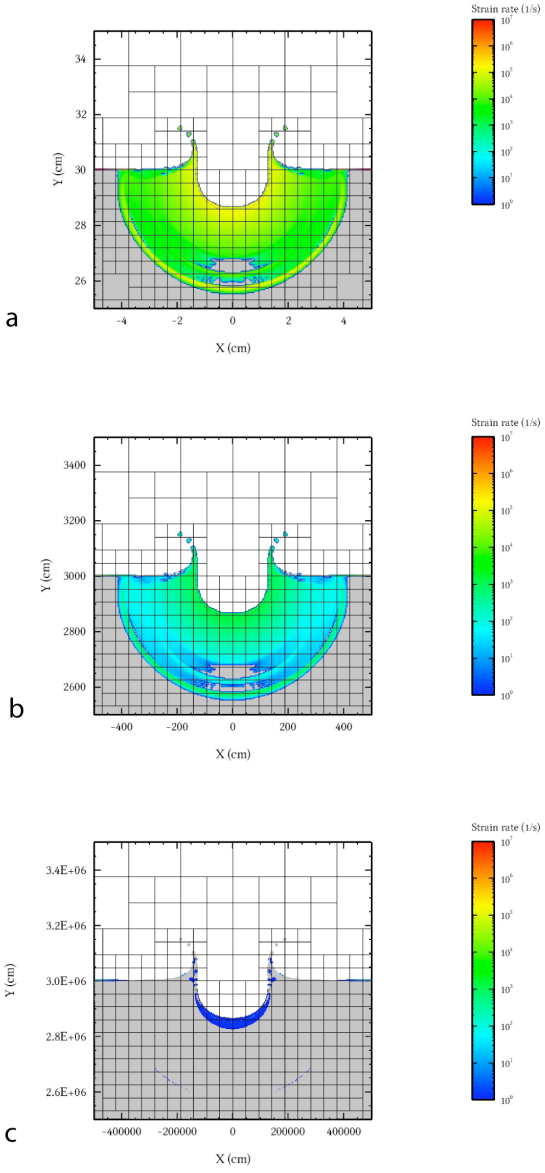

Figure 2. Numerical strain results for impacts of (a) 1 cm at 10^{-5}s, (b) 1 m at 10^{-3}s, and (c) 1 km at 1 s after impact.